Strategies for Immunisation in Inhomogeneous Networks

G. A. Roussos
Department of Mathematics and Applied Mathematics
University of Cape Town
Student ID: RSSGEO005

20 August 2021

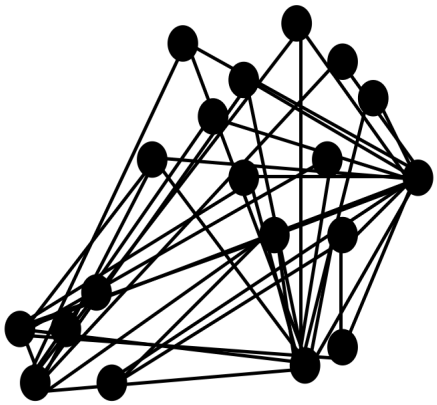

Figure drawn electronically by G. A. Roussos

Abstract

This paper aims to investigate immunisation strategies in a simulated inhomogeneous network. The simulated inhomogeneous network is constructed in three layers. First, individuals are randomly connected in each metropole in South Africa; thereafter, the South African metropoles are constructed as a small world network. In addition, the third layer is constructed by connecting each province as a small world network. The simulations to visualise the random uniform vaccination distribution and an immunisation distribution strategy that targets attractive hubs in the network (regions with a high level of clustering) are programmed in Python. The first strategy investigated was the random uniform distribution of vaccinations. Random uniform immunisation relies on assumptions that are likely to be untrue in reality. Therefore, the second strategy targets movement hubs in South Africa. The immunisation resulting from vaccination is considered to be same for people who have recovered from a disease and is assumed here to have a half-life of 6 months. The results are shown over a time period of 525 time steps in days. The targeted immunisation scheme is shown to produce larger levels of vaccinations than the random uniform immunisation strategy in the same period of time and is concluded to be a more effective scheme for vaccination in South Africa by 25%.

Contents

1 Introduction

Complex networks describe connected maps that display a high level of redundancy and heterogeneity. These particular properties propagate the spread of infectious agents. The aforementioned networks include the interconnectedness of sexual relationships amongst sexually active individuals; the internet, and any social epidemics such as popularised trends and slang and of course, disease epidemics such as the COVID-19 spread. [1]

In March 2020, the emergence of the COVID-19 pandemic took the world by storm. The COVID-19 disease is an infectious respiratory disease caused by a newly discovered coronavirus. Most people infected with the COVID-19 virus will experience mild to moderate illness and recover without requiring special treatment. However, the disease has appeared particularly infectious and as a result has had a severe impact on the health of millions of susceptible individuals. Older people, and those with underlying medical problems like cardiovascular disease, diabetes, chronic respiratory disease, and cancer are more likely to develop serious illness.

Amidst this era of panic, in an attempt to regulate both the number of infected people, and the behaviour of people, governments responded to the pandemic by imposing a series of lockdowns in which the movement of people was restricted to essential travels and international travel was banned all together at one point. This measure used to decrease the rate of contact between individuals had a severe impact on economic growth, mental health and even education. The need to formulate a vaccination and determine the most efficient way to immunise became mandatory.

The aim of the paper was to determine the most efficient strategy for immunisation in an inhomogeneous network, with particular attention to South Africa, where the amount of resources, especially with regard to the healthcare system, is limited. Here, the strategies aiming to achieve global immunisation are explored. Namely, the random uniform immunisation strategy, and the targeted immunisation strategy are investigated first internationally and then, in regard to South Africa. The random uniform immunisation strategy selects a set number of randomly selected individuals globally. In contrast, the discussed targeted immunisation strategy is based on the nodes' connectivity hierarchy. Intuitively, the targeted immunisation strategy seems more efficient in practice and indeed, we can show this to be true.

2 Background Theory

The heterogeneity of the maps is derived from the small path lengths between nodes, and a high degree of local clustering. In laymen's terms, some particular nodes develop a larger probability to create connections in the network. In a scale-free (SF) network the probability follows a power-law distribution in the form:

$$P(k) \sim k^{-\gamma}$$

where P is the probability that a node has k connections. For $2 \leq \gamma \leq 3$, the nodes have a statistically significant probability of having a very large number of connections compared to the average connectivity, $\langle k \rangle$, in a large network. On the contrary, in homogeneous networks, each node has approximately equal numbers of connections, $k \simeq \langle k \rangle$.[1]

So what makes a node more likely to establish connections? According to Malcolm Gladwell, these nodes, or individuals, become the large-scale connectors of a social network. He notes in, "The Tipping Point", that connectors are special types of people who "collect" others, forming increasingly many connections over time. He substantiates this statement by referring to the Syphilis epidemic which occurred in Baltimore, USA, in 1996 and 1997. The STD epidemic was thought to have been propagated by only an increase in drug use in lower-income areas, particularly, in areas in which clinics had recently been defunded. The connectors in this case were people that held a much higher rate of sexual interaction with multiple different people than the average individual. These few connectors link various groups and cliques of very different people as a result of their collective nature. It it easy to see how the spread develops as a function of time.

2.1 Homogenous networks: Random Networks

A network describes a simple object that is defined by a lattice of nodes and links between these nodes. In cases where epidemiological models are investigated, these nodes would describe individuals in which a virus is able to propagate through the network via the links between individuals. This begs the question: how are these nodes distributed in a given network. One obvious way to connect individuals is to randomly place links between them. This leads to the definition of a random network as follows:

A "random network" consists of N nodes where each node pair is connected with probability, p. The construction of the network is a three-staged process. The procedure begins by constructing N isolated nodes. The second step requires selecting a node pair and generating a random number, c, where $0 < c < 1$. If this random number exceeds the probability, p, then connect the selected node pair with a link, otherwise leave the node pair disconnected. The third step is to repeat the second step for all $\frac{N(N-1)}{2}$ node pairs. The network obtained after this procedure is called a random graph or a random network [10]. In this case, the probability that a random network has exactly L is defined by:

$$P_L = \binom{\frac{N(N-1)}{2}}{L} p^L (1-p)^{\frac{N(N-1)}{2}-L}$$

Above, the probability that a random network has exactly L links is the product of three terms. The first is a combinational factor, counting the number of different ways we can place L links among the $\frac{N(N-1)}{2}$ node pairs. This is multiplied by the probability that L of the attempts to connect the node pairs have resulted in a link, p^L. The third factor, $(1-p)^{\frac{N(N-1)}{2}-L}$, describes the probability that the remaining $\frac{N(N-1)}{2} - L$ attempts have generated in a link. [10]

The equation for P_L appears to exhibit the form of a binomial distribution. Thus, we can infer the expected number of links in the network as:

$$\langle L \rangle = \sum_{L=0}^{\frac{N(N-1)}{2}} L P_L = \frac{N(N-1)}{2}$$

In the above, the average probability, p, that a pair of nodes is connected and the number of pairs iterated through.

The expected number of links in a network can be used to determine the average degree of a random network, k, defined as:

$$\langle k \rangle = \frac{2\langle L \rangle}{N} = p(N-1)$$

where $\langle k \rangle$ is the product of the probability, p, that two nodes are connected and $(N-1)$, describing the maximum number of links per node in a network of size N.[10]

2.2 Understanding of Complex networks: Scale-free and Small World Networks

We begin with the Watts-Strogatz (WS) small world network. The model constructs a ring lattice of N nodes each symmetrically connected to k other nodes with k edges. Each edge is then randomly reconstructed with a probability, p, where $p = 1$ represents disorder and $p = 1$ represents regularity. [2]The connectivity of the resulting lattice is distributed exponentially for large k, and an average connectivity $\langle k \rangle = 2K$. It can be generalised that each node has approximately the same number of edges for exponentially bounded networks, $k \simeq \langle k \rangle$. This implies the WS network can be considered a homogeneous map. Furthermore, the average density of infected individuals is

$$\frac{d\rho(t)}{dt} = -\rho(t) + \lambda\langle k \rangle \rho(t)[1-\rho(t)] \tag{1}$$

Wherein density correlations among nodes have been neglected, $-\rho(t)$ describes the unit rate at which a node becomes susceptible, and $\rho(t)[1-\rho(t)]$ describes the average density of newly infected nodes spread by any infected node multiplied by the probability that a given edge connects to a susceptible node. At the stationary point of equation (1), $\frac{d\rho}{dt} = 0$, we see that there exists a nonzero epidemic threshold, $\lambda_c = \langle k \rangle^{-1}$, where:

$$\begin{aligned} \rho &= 0, & \lambda < \lambda_c \\ \rho &\sim \lambda - \lambda_c, & \lambda \geq \lambda_c \end{aligned} \tag{2}$$

If $\lambda \geq \lambda_c$, the spread increases to an epidemic scale. Otherwise, the rate of infection approaches 0.

The dynamics that describe epidemics are characterised by a so called "tipping point": an epidemic threshold. The behaviour that results from an epidemic threshold is identified as an absorbing-state phase transition in critical phenomena. In this case, ρ describes the phase transition, and λ is known as the tuning parameter.

Moreover, the properties of a Strogatz-Watts small world network can be applied to a real-world complex network. A small-world network refers to an ensemble of networks in which the mean geodesic (i.e., shortest-path) distance between nodes increases sufficiently slowly as a function of the number of nodes in the network. The term is often applied to a single network in such a family, and the term "small-world network" is also used frequently to refer specifically to a Watts–Strogatz network.

A network consists of nodes connected by edges. A path in a network is a sequence of alternating nodes and edges that starts with a node and ends with a node such that adjacent nodes and edges in the sequence are incident to each other. Nodes or edges can appear multiple times in the same path, and the number of edges in a path is the length of the path. If a graph is connected, then any node can be reached via a finite-length path starting from any other node. The shortest path between a pair of nodes is called a geodesic path and there can be more than one such path.

Between any pair of nodes in an unweighted network, one can calculate the geodesic distance, which is given by the minimum number of edges that must be traversed to travel from the starting node to the destination node. The number of edges in a path is the length of the path.

A graph's diameter is the maximum of the geodesic distances between node pairs, and the world encapsulated by a graph is "small" if the expected number of hops between two randomly chosen people is small in some sense. In particular, a network is said to be a small-world network (or to satisfy the small-world property) if the mean geodesic distance between pairs of nodes is small relative to the total number of nodes in the network.

The Watts-Strogatz 'Collective dynamics of 'small-world' networks' aims to model dynamical systems as a function of the structure of the environment or "world" in which the system is constructed as opposed to other models that model these systems as functions of time, etc. This is applied to multiple scenarios by the Watts-Strogatz team [2]. One of these systems of particular interest is the viral spreading in a small world. We will investigate the spread and immunisation strategy of the novel coronavirus: COVID-19 using established disease-spread models to estimate the spread locally, and secondly we will evaluate the spread nationally using the graph theory presented in the Watts-Strogatz paper cited[2].

A WS small world network has specific properties and can quantify the characteristics of the graph by the following:

- L(p): path length
- C(p): the clustering coefficient; measures "cliquishness" of a particular region in the map.

To ensure connectivity in the graph, we require that:

$$n \geq k \geq ln(n) \geq 1$$

where $k \geq ln(n)$ guarantees a random mapping.

When these parameters are varied, the following two results emerge:

- A regular lattice ($p = 0$) is highly clustered and demonstrates a large world where L(p) grows linearly with n. In this case: $L \sim \frac{n}{2}k \geq 1$ and $c \sim \frac{3}{4}$ as $p \to 0$.
- A poorly clustered lattered ($p = 1$) demonstrates a small world where L(p) grows logarithmically with n. In this case: $L \approx L_{random} - \frac{ln(n)}{ln(k)}$ and $c \approx c_{random} - \frac{k}{n} \ll 1$ as $p \to 1$.

It is then noted that at the local level, the transition to a small world goes unnoticed $\implies$ even small numbers of short cuts make a small world. To simulate this, a python algorithm was written presenting a scenario whereby the total sample size consists of 30 nodes which we will assume to be individuals/countries/continents that are susceptible to infection. The results can be seen below.

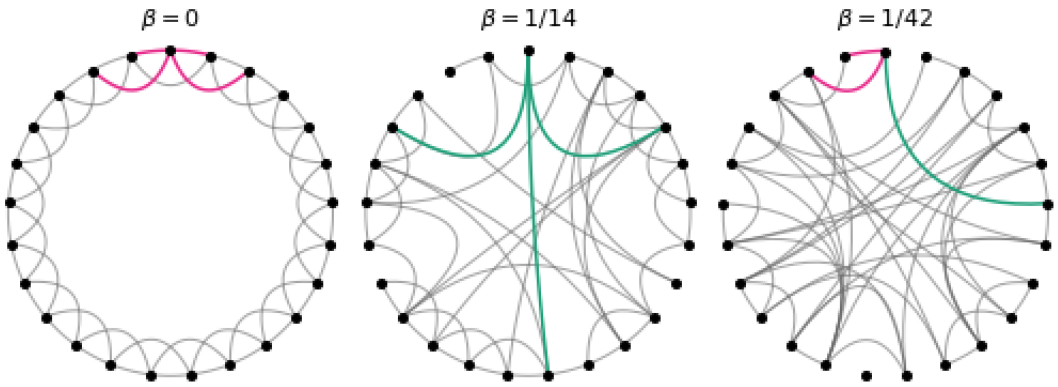

Figure 1: Small-World Network simulated with 30 vertices and a beta value equal to that of COVID-19($\beta = \frac{1}{42}$)

Small-world networks are characterised by local clustering and shortcut ties that reduce the path-length between the clusters. Scale-free networks, on the other hand, take a skewed degree distribution.

Moreover, Scale-Free (SF) networks pose a much harder challenge as the probability distribution, in this case, that a node has a certain number of connections, k, is approximately, $P(k) \sim k^{-\gamma}$. SF networks are modelled as inhomogeneous random graphs. Here, the fluctuations in connectivity among nodes increase exponentially for $2 < \gamma \leq 3$. The classic example of a scale free network is the Barabási and Albert (BA) model where a number, m_0, of isolated nodes is slowly connected by adding m connections to a node with a probability, $\prod(k_i) = \frac{k_i}{\sum_j k_j}$, where k_i describes the connectivity of the i-th node over a series of time steps. The final network obtained is described to have N total nodes where $P(k) \sim k^{-3}$ and the average connectivity in this case is $\langle k \rangle = 2m$. Highly connected nodes of the network are now statistically significant. In addition, there are strong fluctuations in the connectivity distribution of this network. The large fluctuations are taken into account by including the relative density of infected nodes, $\rho_k(t)$, in which case the dynamics of the network is described by the following differential equation: [1]

$$\frac{d\rho_k(t)}{dt} = -\rho_k(t) + \lambda k[1 - \rho_k(t)]\Theta(\rho(t)) \tag{3}$$

where a unity recovery rate is assumed and the probability, $\Theta(\rho(t))$, is defined as $\Theta(\rho(t)) = \frac{\sum_k kP(k)\rho_k(t)}{\sum_s sP(s)}$. In the case described above, a randomly chosen edge is more likely to be linked to a highly connected node that is infected (and therefore, infectious). Thus, it can be shown [1] that the infected node density is related to λ, k and Θ in the following way:

$$\rho_k = \frac{\lambda k\Theta}{1 + \lambda k\Theta}$$

The equation for ρ_k above, can be inserted into equation (3) to formulate the self consistency equation:

$$\Theta = \frac{1}{\langle k \rangle} \sum_k kP(k) \frac{\lambda k\Theta}{1 + \lambda k\Theta}$$

where λ is the only variable. The solution $\Theta = 0$ will always satisfy the self-consistency equation. A prevalence that is non-stationary, $\rho_k \neq 0$, is obtained when both sides of the self-consistency equation are in the interval $0 < \Theta \leq 1$.

This implies that

$$d\Theta\left(\frac{1}{\langle k\rangle}\sum_k kP(k)\frac{\lambda k\Theta}{1+\lambda k\Theta}\right)\geq 1$$

at $\Theta = 0$, corresponding to the critical epidemic threshold, λ_c: [1]

$$\frac{kP(k)\lambda_c k}{\langle k\rangle} = \frac{\langle k^2\rangle}{\langle k\rangle}\lambda_c = 1$$

$$\implies \lambda_c = \frac{\langle k^2\rangle}{\langle k\rangle}$$

The above result indicates that in scale free-networks , where the connectivity exponent is $2 < \gamma \leq 3$ and thus, $\langle k\rangle \to 0$, the critical epidemic threshold is zero, $\lambda_c = 0$. Therefore, for any $\lambda > 0$, the infection can perpetuate through the network with a finite prevalence, in a sufficiently large network with a critical spreading rate that is generalised to SF networks as: [1]

$$\lambda_c(N) = \frac{\langle k\rangle}{\langle k^2\rangle} \sim \frac{1}{\ln(N)}$$

This result can be generalised to SF networks with an arbitrary connectivity distribution, which show an epidemic threshold vanishing as a power law behaviour in N with an exponent depending on the connectivity exponent γ .

2.3 Epidemiological models

Disease spread can be modelled in different ways. In the event of an epidemic, the population can be split into compartments. There will be a susceptible proportion of the population, S, an infected subset, I, and a removed subset resulting from death, R, of the population depending on the model, and finally a vaccinated subset of the population after the development of a vaccine, V. The first model that a disease is able to spread can be described by the SIS model is in which this model describes the disease spread of the virus that has reached the status of being a pandemic. The second way in which a disease spreads can be modelled by the S I R model. The SIS model can be useful in modelling epidemics such as the flu where the rate of death is negligible compared to the rate of infection. However, in order to properly display the population dynamics of infection, death and vaccination the SIR model will be used to simulate the spread of the COVID-19 coronavirus before the development of a vaccine. Thereafter, the SIRV model will be implemented (see section 3.2).

2.3.1 The SIS Model

The SIS model divides the population into two categories defined by the susceptible and infected proportions of the total population. Let S be the number of susceptible individuals, and let I be the number of infected individuals. For an SIS model, infected individuals return to the susceptible class on recovery because the disease confers no immunity against reinfection. This model is used to study the dynamics of epidemics where the rate of mutation of the virus is too fast to build an immunity to a strain of the virus. This appears to be the case for common ailments such as the common flu, and the coronavirus is lightly to take on this model in the coming years as the death rate decreases and vaccination has proved to be effective. The SIS model is defined by the following set of differential equations:

$$\frac{dS}{dt} = -\beta SI + \alpha I$$

$$\frac{dI}{dt} = \beta SI - \alpha I$$

Here, βSI is described to be the average number of infected individual that makes sufficient contact to infect βN others per unit of time. The probability that an individual exposed to the disease is susceptible is S/N. Therefore, if an individual is infected they will spread $(\beta N)(S/N) = \beta S$ infections per unit time and the collective group of I infected individuals cause a total number of βSI infections per unit time. Furthermore, α is the fraction of infected individuals who recover and become susceptible once again per unit time.

$$\frac{d}{dt}(S + I) = 0,$$

so

$$S + I = N = \text{constant}.$$

Here N is the total population. Substituting $I = N - S$ into the second differential equation above, it can be seen that: $\frac{dI}{dt} = \beta I(N - I) - \alpha I = (\beta N - \alpha)I - \beta I^2$.

Solving $dI/dt = 0$, we see that there are two possible equilibria for this SIS model, one with $I = 0$ and the other with $I = N - \alpha/\beta$. Defining the basic reproductive number as

$$R_0 \equiv \frac{\beta N}{\alpha},$$

it can be shown that $R_0 < 1 \Rightarrow$ the equilibrium with $I = 0$ is stable, $R_0 > 1 \Rightarrow$ the equilibrium with $I = N - \alpha/\beta$ is stable. [3]

Immunisation regimes are often based on the SIS (susceptible-infected-susceptible) model. Here, each node describes an individual and each node is connected by a varying number of links along which the infection is able to spread. A susceptible node is infected with a rate, ν, if it has connections to one or more nodes. Furthermore, infected nodes once again become susceptible with a rate, δ. Thus, the effective spread rate is defined as $\lambda = \frac{\nu}{\delta}$. For simplicity's sake, and without lack of generality, δ is set to 1. The SIS model model does not consider a person's removal from the system as a result of death or acquired immunisation. Thus, individuals will run cyclically through being susceptible, being infected and then being susceptible again. Spreads of infection leading to endemic states have a stationary average density of infected individuals, thus, the SIS model is appropriate in this case.

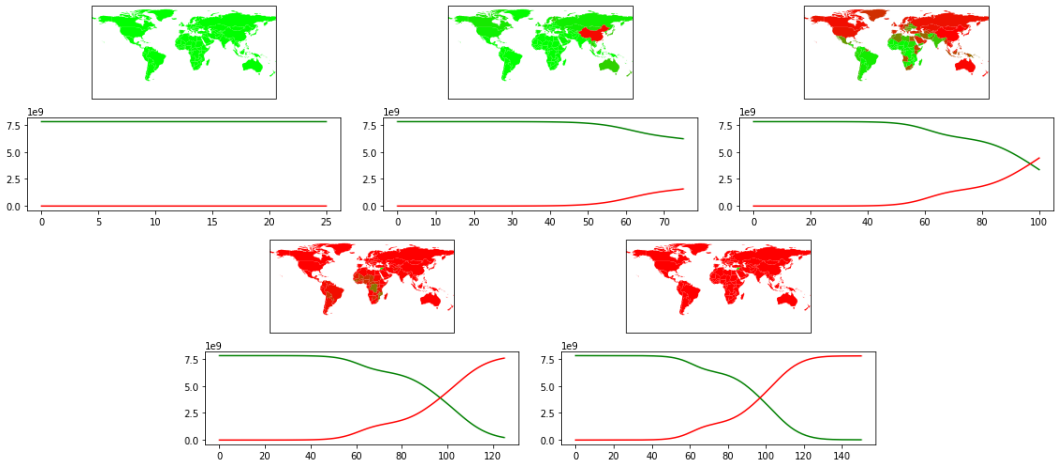

Figure 2: SIS simulation of the global spread of COVID-19 implemented in python with data found from *OurWorldInData* at the 25th, 75th, 100th, 125th and 150th respectively

2.3.2 The SIR Model

W. Kermack and A. McKendrick created a new epidemiological model in which they considered a fixed population with three subsets of the population: susceptible, $S(t)$; infected, $I(t)$; and recovered, $R(t)$. Again, $S(t)$ is used here to represent the individuals not yet infected with the disease at time t, or the subset that is susceptible to the disease of the population. $I(t)$ represents s the individuals of the population who have been infected with the disease and are capable of spreading the the susceptible subset of the population. Finally, $R(t)$ is used to describe the compartment of the individuals of the population who have been infected and then removed from the disease, either due to immunisation or death. The people who fall in this removed category can no longer transmit or contract the disease at hand. The model will iterate through individuals where each person will be susceptible then infected and possibly removed from the network, depending on the death rate of the disease. [11]

Furthermore, in a fixed population the dynamics of the system are conserved, i.e. $N = S(t) + I(t) + R(t)$. The model has initial conditions that describe the number of people in the susceptible, infected and removed categories at the first time step: $S(0) = S_0$, $I(0) = I_0$, $R(0) = R_0$. If the SIR model is assumed to describe the dynamics of the system at all values of time, t, then the initial conditions described are not independent. The simulation first updates the infected individuals from the susceptible portion of the population and then the removed subset is updated from the infected subset for the next time step, thus, the flow of the system is first from susceptible to infected to removed. The death rate of the disease, γ and the infection rate, β, determine the length of the epidemic and change over the course of disease outbreak but these parameters will be kept constant. The susceptible, the infected and the removed subsets of the population encapsulate the death rate of the disease, γ, and the infection rate, β in the following way: [11]

$$\begin{aligned} \frac{dS}{dt} &= -\frac{\beta SI}{N} \\ \frac{dI}{dt} &= \frac{\beta SI}{N} - \gamma I \\ \frac{dR}{dt} &= \gamma I \end{aligned} \tag{4}$$

However, there are multiple assumptions made when we construct the SIR model. The first is that an individual is considered to have to same probability as any other individual in the system of contracting the disease with a rate a and, that there is an equal fraction b of people that an individual makes contact with in one time step in the SIR simulation. From this, we see that the rate of infection, β is the multiplication of a and b, i.e. β the multiplication of the transmission probability times the contact rate. Here, an infected individual makes contact with b people in a time step, however, only $\frac{S}{N}$ of these contacts are susceptible and able to contract the disease. Therefore, the total subset of infected individuals can infect $abS = \beta S$ susceptible individuals, thus, the number of susceptible people infected by the I subset of the population is βSI in one time step. The second and third differential equations above describe the subset of individuals leaving the susceptible class as equal to the number of newly infected individuals. Furthermore, a fraction of infected individuals, γ, is prescribed to leave the infected class and enter the removed subset of the population per unit time. These processes which occur simultaneously are referred to as the Law of Mass Action, a widely accepted idea that the rate of contact between two groups in a population is proportional to the size of each of the groups concerned. Finally, it is assumed that the rate of infection and recovery is much faster than the time scale of births and deaths and therefore, these factors are ignored in this model [11].

Similarly, we can build an immunisation strategy on the population dynamics that govern the SIR (susceptible-infected-removed) model. Again, each node describes an individual and each node is connected by a varying number of links along which the infection is able to spread. A susceptible node is infected with a rate, ν, if it has connections to one or more nodes. Furthermore, infected nodes once again become susceptible with a rate, δ. Thus, the effective spread rate is defined as $\lambda = \frac{\nu}{\delta}$. Here, δ is set to approximately 12 months if we consider immunisation from vaccination. On the contrary to SIS population dynamics, the SIR model does consider a person's removal from the system (specifically in this case it would be death if we plan to construct a immunised class of individuals).

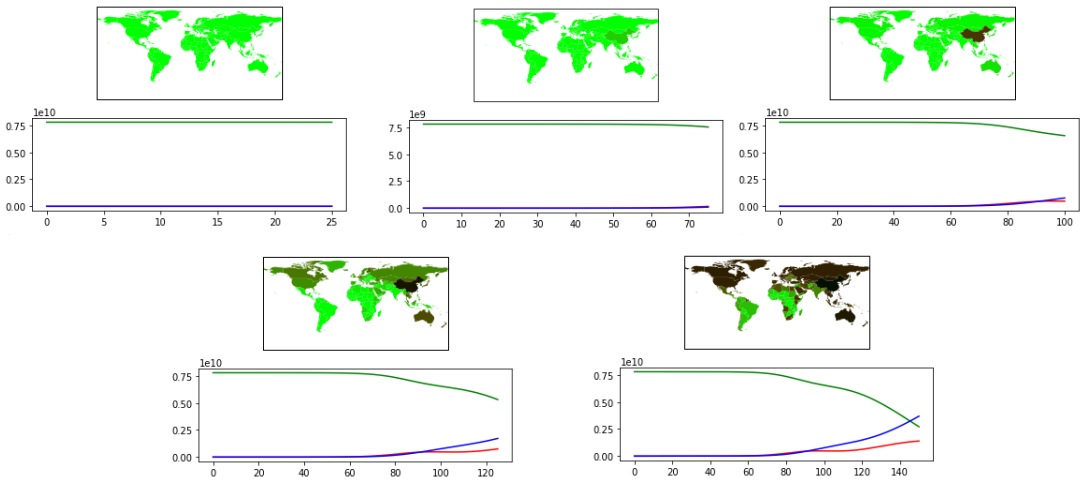

Figure 3: SIR simulation of the global spread of COVID-19 implemented in python with data found from *OurWorldInData* at the 25th, 75th, 100th, 125th and 150th respectively

2.4 Strategies for Immunisation of Inhomogeneous Networks

We will explore two strategies for the immunisation of the inhomogeneous network. Foremost, the random uniform immunisation strategy is implemented globally in a homogeneous network and discussed. The second scheme discussed

is a targeted immunisation strategy within South Africa relative to the population. This is done to determine if targeting population hubs for vaccination is more time and cost effective than other strategies such as targeting the immunisation of individuals randomly.

2.4.1 Random Uniform Immunisation

The random uniform distribution of vaccines is the simplest immunisation strategy whereby a random selection of a fixed number of individuals is immunised at a constant rate. This random uniform immunisation regime is based on the SIS epidemiological model. In homogeneous small-world networks, the prevalence becomes stationary with a constant spreading rate, λ, and is given by:

$$\rho = 0, \quad g > g_c$$

$$\rho \sim g_c - g, \quad g \leq g_c$$

where g_c is the critical immunisation and is defined in terms of λ as: $g_c = \frac{\lambda - \lambda_c}{\lambda}$. Thus, the critical immunisation which achieves total immunisation is related to the spreading rate and the epidemic threshold of the infection for $\lambda > \lambda_c$. This is shown in the results section for a global mapping. The regime would be effective if our system was homogeneous. However, due to the complexity that arises in real-life scenarios, it is necessary to increase the heterogeneity of the network by adding tiers of random and small-world mappings.

The uniform random distribution randomly selects gN nodes from the susceptible pool of nodes and identifies a new class of immunised nodes that cannot become infected, and are no longer susceptible. However, it is necessary to ask what it means for a node to become immunised. The vertices of the network are described in this case to be airports each connected with a power-law distribution. But how can we assume a whole airport is to be immunised instantaneously? The assumption of instantaneous immunisation of a node(an "airport") is therefore, inapplicable to a global case as the network requires a rate of immunisation/a rate of vaccination instead of assuming the entire node is immunised in a single time step. The simulation cited in the Pastor-Satorras et al. reference paper, runs through network sizes of $N = 10^4$ to $N = 10^6$. However, within the limitations of the sourced data, the number of nodes in the constructed network is much less than this. We therefore include uniform immunisation distribution per individual in each country which are randomly selected from the susceptible pool of the country at each time step with a constant rate of vaccination. However, how fair is the assumption that flights are operating at maximum capacity in the middle of a pandemic? The ideal model would also include a decay rate of plane capacity as the number of infections increases but this is beyond the scope of the paper.

The figures for the random uniform immunisation strategies are shown below. The first figure as at the 25th time is that the second is at the 50th time step and the third is that the 75th time step. Here, the SIS model is used because COVID-19 has been declared a pandemic by the World Health Organisation (WHO) in 2020.

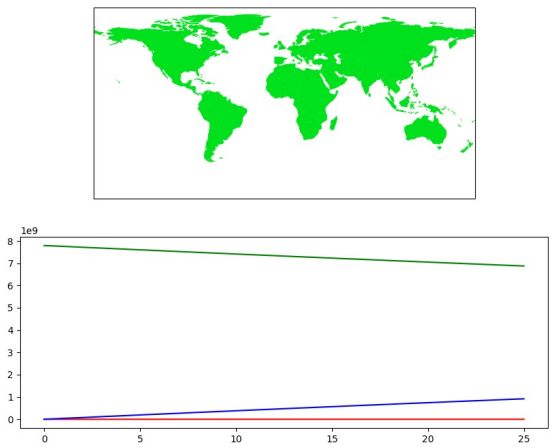

Figure 4: The figure depicts random uniform immunisation performed locally (on an individual level) based on an SIS model of infection spread at the 25th time-step presented as a global map. The map is coloured light green indicating that the global population is healthy at the 25th time-step. The red curve, below, represents the number of people infected, the green curve represents the total number of susceptible people as a function of time, and the blue curve describes the number of immunised individuals from $t_0 = 0$ to $t = 25$ weeks

In figure (4) above, we see that the number of infected people and has become static over time and the number of vaccinated people has increased steadily as expected for the random uniform immunisation strategy. In addition the number of susceptible people has decreased steadily proportionately to the number of people vaccinated.

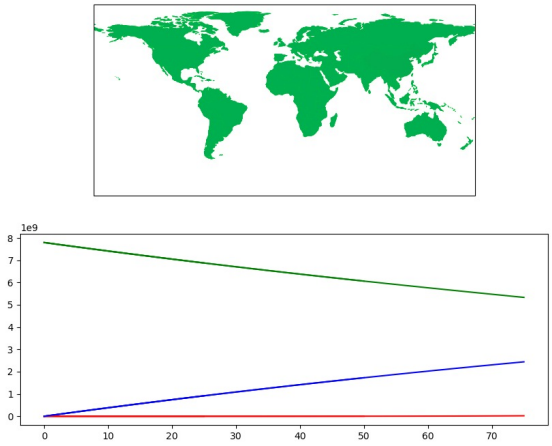

Figure 5: The figure depicts random uniform immunisation performed locally (on an individual level) over the SIS model at the 75th time-step presented as a global map. The map is coloured a dark green indicating that the global population is 25% immunised. The red curve, below, represents the number of people infected, the green curve represents the total number of susceptible people as a function of time, and the blue curve describes the number of immunised individuals from $t_0 = 0$ to $t = 75$ weeks.

Secondly, figure (5) shows that this trend has progressed and we see that approximately a quarter of the population has been vaccinated. We see again that the number of people infected has approximately remain constant overtime. However, a vaccination rate of 5% per day globally is an unrealistic immunisation rate when we consider the cost of distribution. It is unlikely that this rate would be able to be maintained globally for the course of the epidemic. Thus, there needs to be a more efficient strategy to distribute these vaccinations within cost and time limitations. This leads us to the targeted immunisation strategy.

2.4.2 Targeted Immunisation: Targeting Hubs

Now we consider if a fraction, g of the individuals with the highest connectivity is immunised with a immunisation half-life of 6 months . That is, if a person gains partial immunisation from infection or vaccination, the time in which the individual will be completely susceptible again is approximately one year. Complete immunisation is assumed to be unachievable thus the 'immunised' class becomes a second susceptible class in the SIR model, but this particular population is less susceptible than completely 'healthy' individuals. This fraction of highly connected individuals introduces a threshold for the connectivity k_t such that $k > k_t$ have been immunised.[1] The fraction of individuals is given by:

$$g = \sum_{k<k_t} P(k)$$

and the approximate solution for the immunisation threshold for targeted immunisation is:

$$g_c \approx e^{\frac{-2}{m\lambda}}$$

Furthermore, the targeted immunisation was implemented by simulating the SIR model on the WS and BA networks

within South Africa, its provinces and its metropoles, by immunising gN nodes with the highest connectivity. Here, the rate of disease spread is taken to be fixed over time.

3 Model Methods & Data Sourcing

3.1 Network Construction

The model was constructed using a three-tiered network. Foremost, individuals located in South African Metropoles were connected randomly within the district or metropole. The number of each individuals/nodes in each metropole network is equal to the population of that city defined in the `za_areas` excel files [6].

At the local level, the model constructs a network that is nearly homogeneous. Clustering at the local level, is therefore, less prevalent. Inhomogeneity is considered in the second tier of the network model whereby the metropoles of South Africa were constructed as a small world network (WS small world network). Thereafter, we can extend this with increasing inhomogeneity, to model each province connected in country-wide small world network. These city populations are constructed on a Python map [7] as seen in figure (6) below overlapped with a geographic picture of South Africa cited from [8].

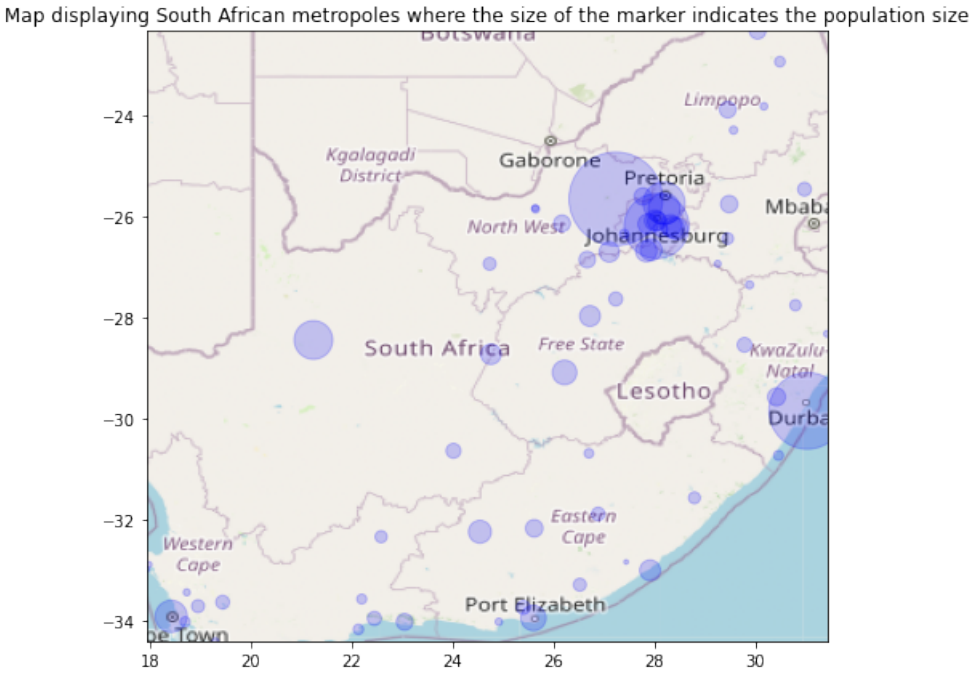

Figure 6: Bubble map of South Africa depicting the metropoles of South Africa whereby the size of the bubble indicates the size of the population of the cities.

Furthermore, defining the movement in the network such that individuals would be able to travel within the 3 lays of the network is not an easy task. The way that the internal movement was constructed started at the local level whereby an individual located in any metropole is able to travel to the cities within their province or any capital city in South Africa (thus, if the individual is travelling to capital city, they would be travelling to a new province). This constructs a 3 tiered network as desired. An individual can randomly interact with anyone in their current city and can only move across the nation via a finite set of trajectories. The maximum length of the trajectory of an individual was assumed to be 4, meaning that an individual can travel to any 4 valid destinations before they are forced to go home (to their home city). The list of valid destinations that an individual located in any city is allowed to take is located in the appendix at the end of the paper.

3.2 The SIRV Model & The Targeted Immunisation Strategy

The vaccination strategy was based on the SIR model. To consider partial immunisation due to vaccination regimes, a second susceptible class S_v is added and describes the pool of individuals that have been that have been immunised. This immunisation is assumed to have a half-life of 6 months. The SIRS_v model, in practice, will assume that S_v is the number of people that have been vaccinated. For simplicity's sake, S_v will be denoted as V, for the number of vaccinated individuals in the population.

This model compartmentalises the population into 4 classes: the susceptible portion of the population, S, the infected individuals in the network, I, the recovered individuals, R, and vaccinated people in the sample population, V. These variables, S I R V, are functions of time, i.e. $S = S(t), I = I(t), R = R(t), V = V(t)$. The SIRV model is governed by the following set of differential equations [5]:

$$\dot{S(t)} = \mu - (\mu + u(t))S(t) - \beta S(t)I(t) + \phi V(t) + \nu R(t)$$
$$\dot{I(t)} = \beta S(t)I(t) + \sigma\beta V(t)I(t) - (\mu + \gamma)I(t)$$
$$\dot{R(t)} = \gamma I(t) - (\mu + \nu)R(t)$$
$$\dot{V(t)} = u(t)S(t) - (\mu + \phi)V(t) - \sigma\beta V(t)I(t)$$

where β is the transmission rate, μ is the death rate, γ is the recovery rate, ν is the rate of immunity loss, $u(t)$ is the vaccination rate, and ϕ is the vaccination waning [5]. The initial conditions of the SIRV model are

$$S(0) = S_0, \;\; I(0) = I_0, \;\; R(0) = R_0, \;\; V(0) = V_0$$

and, since the death rate is equal to the birth rate, the system is closed, i.e. $S(t) + I(t) + R(t) + V(t) = 1$. The vaccination scheme in the model was only implemented after the 365th day (the 365th time step) approximately one year after the start of the epidemic. Before the 365th time step, the SIR model was used to simulate the spread before the development of a vaccine.

Furthermore, the vaccination strategy implemented in the paper was to target hubs of movement within South Africa (section 2.4.2). These results are compared to a random uniform immunisation strategy (section 2.4.1) to determine which is the most effective scheme for vaccination in South Africa.

3.3 Algorithm Construction

To construct the above network and vaccination scheme, we begin the code by initialising the South African metropoles and determining their given populations and areas in the data file [6]. We then plot the South African map indicating areas of habilitation where the size of the marker indicates the size of the city population. Each metropole in the algorithm contains the number of nodes that corresponds to the population of the city. The nodes describe individuals as follows:

```
individual = {
        "home_city": home_city,
        "current_province": current_province,
        "status": status,
        "trajectory": trajectory,
        "going_home": going_home,
        "id": _id,
    }
```

In the above, we have defined the current city, the current province, the status of the individual (being susceptible, infected, removed or vaccinated), the trajectory of the individual (defined as a `numpy` array), a function that defines

when the individual is forced to go home and the identity number of the individual in the simulation. Next, internal movement between provinces is defined whereby an individual has the aforementioned attributes:

```
if individual["trajectory"][-1] in capitals:
    valid_destination = cities[individual["current_province"]] | capitals
else:
    valid_destination = cities[individual["current_province"]]

next_city = random.choice(tuple(valid_destination))  # Uniform distribution

if next_city == individual["home_city"]:
    tracjectory = [individual["home_city"]]

elif next_city == individual["trajectory"][-1]:
    pass

else:
    individual["trajectory"].append(next_city)
    province_idx = [
        next_city in p_cities for _, p_cities in cities.items()
    ].index(True)
    individual["current_province"] = list(cities.keys())[province_idx]

if len(individual["trajectory"]) > 4:
    individual["going_home"] = True
else:
    home_or_not = [True, False]
    individual["going_home"] = random.choice(home_or_not)
```

The nest step in the algorithm construction is to store the set of cities in each province of South Africa in order to determine the trajectory of an individual within a province moving between neighbouring cities and between the capitals of South Africa. A person is able to move between provinces by travelling to admin Capitals in each province and then allowed to move within that prospective province. The maximum length of the trajectory is the maximum number of internal movements before an individual is forced to go home.

Thereafter, the SIR model is imposed on the movement network and the disease is able to spread from individual to individual where this spread is dictated by the individual trajectories between metropoles. At the 365th time step, a year after the outbreak of the disease in the simulation, the targeted immunisation scheme is implemented to determine if targeting hubs is a more effective vaccination scheme. The vaccination data is included by proportionately vaccinating people in each city South Africa relative to the population size of the city, the size of the inverse of the population and randomly as follows:

```
if t > VACCINATE_THRSH:
```

```
total_sus = iteration_stats["total"]["susceptible"]

random_dist = np.random.random(len(df))
random_dist /= random_dist.sum()
if total_sus != 0:
    for i, city in enumerate(df.city):
        if VAX_STRAT == "high_first":
            num_vaccines = MAX_VAX*iteration_stats[city]["susceptible"]/total_sus
        elif VAX_STRAT == "low_first":
            num_vaccines = MAX_VAX*(1-iteration_stats[city]["susceptible"]/total_sus)
        else:
            num_vaccines = MAX_VAX*random_dist[i]

        num_vaccines = min(int(num_vaccines), iteration_stats[city]["susceptible"])
```

These results are plotted in a time series of maps as seen in the results section of this paper.

3.4 Data Sourcing

The data set for the proposed targeted immunisation of the three tiered network comprised of the population data; the COVID vaccination data and the total number of COVID confirmed cases of each district within South Africa, the approximate geo-location of each district and the geolocations of each province. The population data can be sourced from `http://www.statssa.gov.za/`, otherwise, a list of South African metropoles and their populations is given in [6]. The number of vaccinations and confirmed cases can be found in csv format in the following GitHub repository: `https://github.com/CSSEGISandData/COVID-19`. South Africa has an average vaccination distribution per day of 100 000 vaccines. Finally, the geo-data was determined using the latitudes and longitudes defined in [6] and visualised in a series of maps constructed via the method proposed in [7]. These cities were superimposed on a map of South Africa [8].

The population data is scaled down due to CPU running-time constraints. Without scaling down, the python algorithms collectively take approximately 80 hours to run. The sample population is 15 194 400 individuals. These people are simulated as nodes in an inhomogeneous network, compared to South Africa's current population of approximately 59 310 000. The sample network is then scaled down by 100 leaving the simulation running with a total of 151 944 nodes in the network. The scaled down sample population allows the python algorithm to run in a much faster time period of approximately an hour and a half. A scaled down population is able to accurately simulate the dynamics of the immunisation strategy provided that the parameters of the system are scaled appropriately too. It is a difficult task to solve for these parameter scalings, but it is possible with a trial-and-error process. The maximum number of vaccinations of 100 000 is also scaled down as a result of the sample size of the simulation. As long as we are able to depict the dynamics of both vaccination systems, these scalings are negligible.

4 Results and Discussion

The results of the algorithm presented above are displayed in a time series of bubble maps indicating the population percentage of vaccinated individuals from the 375th time step to the 525th time step. We begin at the 375th time step because it is approximately 10 days after the vaccination distribution has begun in the simulation. For this reason, it is an ideal time step to begin to visualise the vaccination distribution across South Africa. The random immunisation strategy will be presented first followed by a targeted scheme in which attractive hubs are prioritised. These results are discussed as the simulation progresses.

All codes are written in Python Jupyter Notebooks located at the following Github repository:
`https://github.com/georgiroussos/Strageties-for-Immunisation-in-Inhomogeneous-Networks`

4.1 Random Uniform Immunisation

The random uniform strategy for vaccination was simulated in python over the network defined in section (3.1). The results can be seen below in figures (7)-(10) below for the 375th, 425th, 475th and 525th time step. Figure (7) can be seen below:

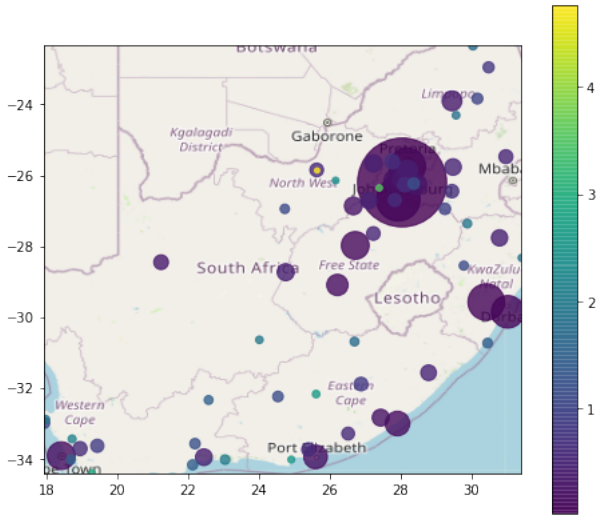

Figure 7: Colour-map depicting the percentage of people vaccinated in each metropole at the 375th simulation time-step where the size of the marker indicates the population size of the city. The total number of vaccinated people in the 375th time step using the random uniform distribution is 4659 individuals.

In figure (7) the map depicts the percentage of vaccinated individuals at the 375th time step (approximately 10 days after the start of the distribution of vaccines using random uniform immunisation strategy). In the figure, we see that the majority of cities have a percentage of vaccinated individuals of less than 1% per metropole at this time step. Only two cities in the North West province has a vaccination percentage of more than 3%.

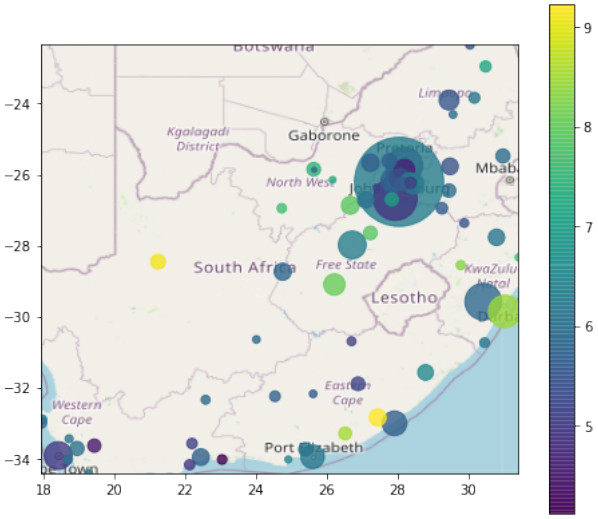

Figure 8: Colour-map depicting the percentage of people vaccinated in each metropole at the 425th simulation time-step where the size of the marker indicates the population size of the city. The total number of vaccinated people in the 425th time step using the random uniform distribution is 28007 individuals.

Secondly, in figure (8), the average percentage of vaccinations at the 425th time step (the 425th day in the simulation approximately 60 days after the start of the random uniform vaccine distribution) of 5.8%. One is now able to see that the distribution is random as there seems to be no correlation between the vaccination percentages of adjacent cities.

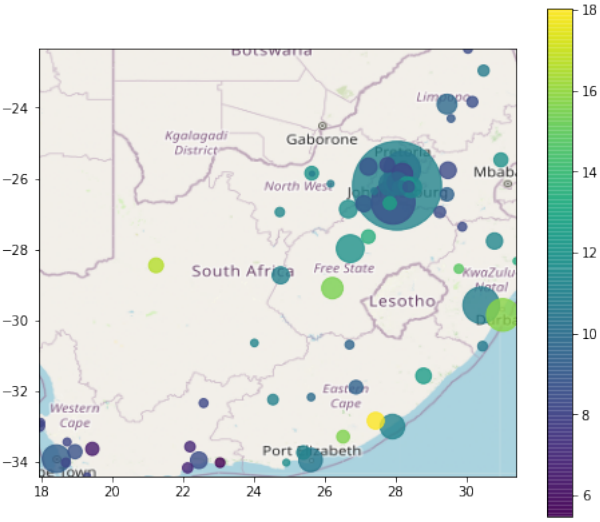

Figure 9: Colour-map depicting the percentage of people vaccinated in each metropole at the 475th simulation time-step where the size of the marker indicates the population size of the city. The total number of vaccinated people in the 475th time step using the random uniform distribution is 46978 individuals.

Furthermore, in figure (9), the average percentage of vaccinations at the 475th time step (the 475th day in the simulation approximately 110 days after the start of the random uniform vaccine distribution) of 10.4%. The randomness of the percentage of vaccinated individuals has increased in the graph.

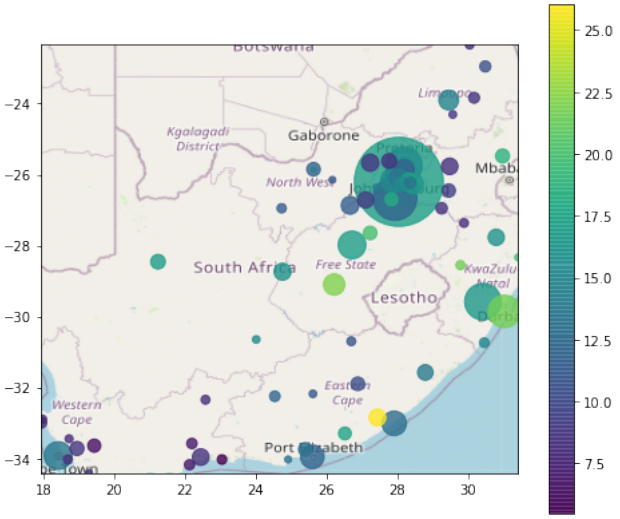

Figure 10: Colour-map depicting the percentage of people vaccinated in each metropole at the 525th simulation time-step where the size of the marker indicates the population size of the city. The total number of vaccinated people in the 525th time step using the random uniform distribution is 57954 individuals.

Lastly, in figure (10), the average percentage of vaccinations at the 525th time step (the 525th day in the simulation approximately 160 days after the start of the random uniform vaccine distribution) of 14.9%. The graph appears totally random with no correlation between the percentage of vaccinated individuals of adjacent cities in South Africa.

4.2 Targeted Immunisation within South Africa

In most real life networks, we cannot assume such a high rate of vaccination and thus the only way to properly vaccinate is through proportional immunisation strategies. In this section we explore the proportional immunisation strategy relative to the Metropole population size. This strategy will be implemented by first targeting population-dense areas. The aim of the paper is to determine if targeting metropoles is a faster mechanism to immunise a population than by randomly distributing vaccines by comparing the results presented below to that presented for the random immunisation scheme above.

On August 5, 2021, South Africa administered 126,353 doses of vaccine against the coronavirus (COVID-19). The country started the vaccination campaign on February 17, 2021, with the first 1,130 doses from Johnson & Johnson. The country actually begun its vaccination program by securing one million AstraZeneca/Oxford in Feburary 2021. Thereafter, these injections were retracted after discovering their ineffectiveness towards the more contagious new variant of the Covid-19 virus that spread in tSouth Africa. South Africa has ordered 11 million doses of the Johnson & Johnson single-shot vaccines as well as 20 million doses from Pfizer. Moreover, the country has reached an agreement with the United Nations to receive 12 million vaccine doses. [4] The maximum number of vaccines per day is the average number of distributed vaccines nationally and is approximately equal to 100 00. Since our population size is smaller than the total population of South Africa, this maximum number is scaled down to 25000.

Foremost, we explore an immunisation strategy defined by selecting gN nodes of the population is with the highest connectivity first. We then select GN nodes in metropoles with the lowest connectivity and then randomly across

metropoles, to ultimately interpret if distributing vaccinations to dense populations first is more effective than random immunisation. The results are presented in figures (11)-(14) below:

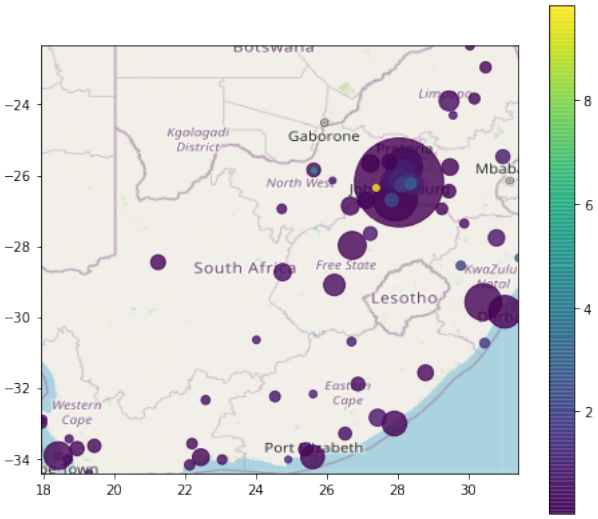

Figure 11: Colour-map depicting the percentage of people vaccinated in each metropole at the 375th simulation time-step where the size of the marker indicates the population size of the city. The total number of vaccinated people in the 375th time step using a targeted immunisation distribution is 4677 individuals.

Foremost, in figure (11), the average percentage of vaccinations at the 375th time step (the 375th day in the simulation approximately 10 days after the start of the targeted vaccine distribution) of just under 1%. This is approximately the same as the random uniform distribution at the first displayed time step map in figure (7).

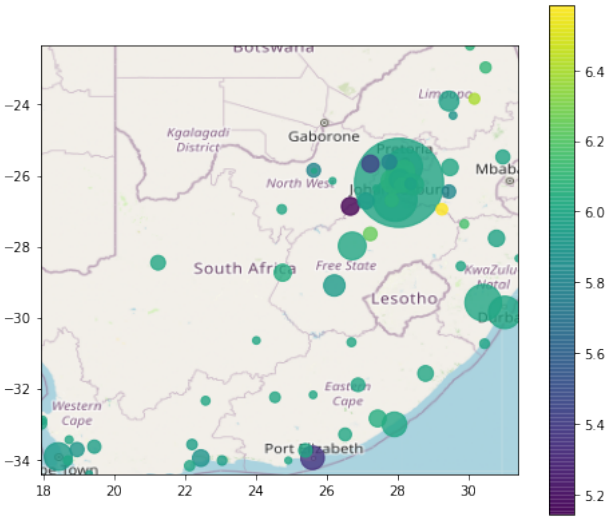

Figure 12: Colour-map depicting the percentage of people vaccinated in each metropole at the 425th simulation time-step where the size of the marker indicates the population size of the city. The total number of vaccinated people in the 425th time step using a targeted immunisation distribution is 28076 individuals.

Secondly, in figure (12), the average percentage of vaccinations at the 425th time step (the 425th day in the simulation approximately 60 days after the start of the random uniform vaccine distribution) of 6.0%. This is 0.2% higher using

the same number of vaccinations per day than the percentage of individuals vaccinated using the random uniform immunisation scheme. The targeted scheme starts to present a more efficient distribution of vaccines as the figure displays that the number of vaccines distributed to a city is proportional to the size of the province small-world network. In addition, adjacent cities appear to have a correlated percentage of vaccinated individuals depending on the movement of individuals.

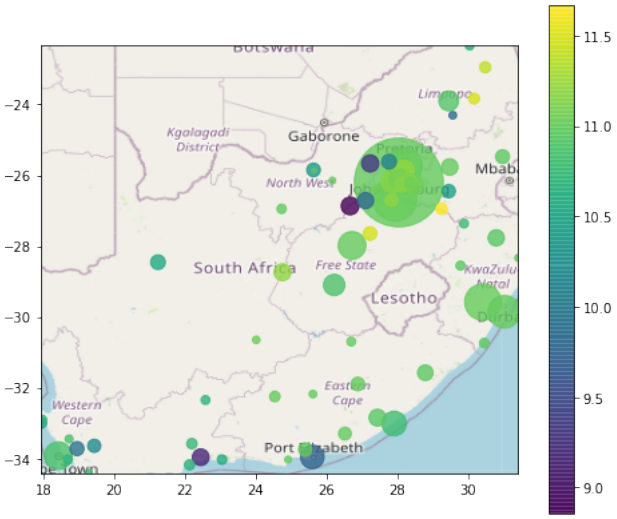

Figure 13: Colour-map depicting the percentage of people vaccinated in each metropole at the 475th simulation time-step where the size of the marker indicates the population size of the city. The total number of vaccinated people in the 475th time step using a targeted immunisation distribution is 51415 individuals.

Furthermore, in figure (13), the average percentage of vaccinations at the 475th time step (the 475th day in the simulation approximately 110 days after the start of the random uniform vaccine distribution) of 11.0%. This percentage is approximately 0.4% larger than the percentage of individuals vaccinated using the random uniform immunisation scheme at the same time step.

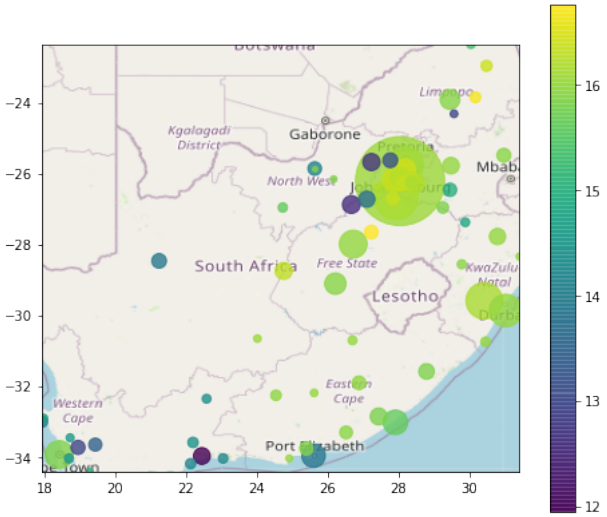

Figure 14: Colour-map depicting the percentage of people vaccinated in each metropole at the 525th simulation time-step where the size of the marker indicates the population size of the city. The total number of vaccinated people in the 525th time step using a targeted immunisation distribution is 74623 individuals.

Lastly, in figure (14), the average percentage of vaccinations at the 525th time step (the 525th day in the simulation approximately 160 days after the start of the random uniform vaccine distribution) of 15.9%. This percentage is approximately 1.0% larger than the percentage of individuals vaccinated using the random uniform immunisation scheme at the same time step. This translates to approximately 1500 more vaccinations given using the targeted scheme as opposed to the random uniform distribution. In addition, the total number of vaccinations given at this time step using the targeted immunisation strategy is 74623 individuals, whereas the random uniform distribution gives a total number of vaccinations of 57954 individuals.

Therefore, the percentage difference between the number of vaccinations at the 525th time step of the random uniform distribution scheme and the targeted distribution scheme is 25.1%. Thus, the strategy to prioritise the immunisation of movement hubs in South Africa is 25.1% more efficient than vaccinating randomly in an inhomogeneous network like the network defined above.

4.3 Remarks & Limitations

Despite being able to simulate the spread of COVID-19 in South Africa the given targeted model has a number of limitations that may affect the outcome of the results. Foremost, the model assumes that the immunisation from a vaccine and the immunisation resulting after infection is the same. The second limitation of the model is that the spreading rate is taken to be fixed throughout time. The third limitation is at the rate of daily vaccination is taken to be fixed as well; because we had taken a sample of the population, the sample size is a quarter of the true population of South Africa and although it may display the correct relationship and rate of vaccination, the results may not be accurate.

Foremost, the model assumes that immunisation from a vaccine is the same level of immunisation that occurs from infection. This has been shown not to be true by the World Health Organisation and that immunisation from vac-

cination is stronger than that from infection. Immunity from natural infection starts to decline after 6 to 8 months; fully vaccinated individuals people still have sufficient immunity after a year [9].

Secondly, the model assumes that the rate of spread of the COVID-19 coronavirus is constant. The spread of the respiratory disease is dependent on the rate of contact between individuals and the inherent infectiousness of the disease. The rate of contact between individuals is, in fact, a function of time that depends on the rate on contact and can be decreased by governmental interventions such as mandatory sanitising stations and national lockdown strategies. These factors are not included in the model and may indicate the vaccination in the model is required to start earlier than a real-life epidemic.

Lastly, the rate of daily vaccination is also taken to be fixed throughout time. This rate is dependent on the availability of vaccinations and the number of susceptible people that still need to be vaccinated. The model, however, assumes this rate is constant and thus, the dynamics of the models present an ideal, constant supply of vaccinations which, in the real-world, is likely to be untrue.

Therefore, even though the simulation is able to depict the dynamics of each immunisation strategy in an inhomogeneous network, the limitations of the model presented above may hinder the accuracy of both simulations. However, since these assumptions are made in both immunisation strategies, their results can safely be compared. A final remark considers the vaccination strategies of South Africa. The South African government implemented an age-tiered vaccination distribution scheme, but because the dynamics of this scheme can be implemented randomly or we can target hubs and age, however, this is beyond the scope of the project.

5 Conclusions

In conclusion, we have simulated and visualised different strategies of immunisation in inhomogeneous networks: the random uniform immunisation strategy and a targeted immunisation strategy in which attractive hubs in the network are prioritised for vaccination. The network was constructed by allowing an individual to travel to neighbouring cities within a province and to capital cities in different provinces. This creates a three tiered network the first layer is a random distribution of individuals, the second tier is a small world network in between cities within a province; and finally, the third layer is a small network between provinces which are defined by capital cities in the simulation. The uniform immunisation strategy has only shown to work for large rates of vaccination and although the results present adequate estimations of the number of people that should be vaccinated per day, the vaccines should be distributed in a different way to increase the efficiency of the vaccination scheme in the inhomogeneous network defined in the project. We then investigate a targeted immunisation strategy within South Africa whereby attractive hubs in the network are prioritised in the distribution of vaccines. The random uniform distribution strategy is shown to perform less efficiently than the targeted scheme by 25%. Therefore, it can be concluded that with the same daily rate of vaccination, and the same disease parameters, the targeted scheme is a more efficient immunisation strategy for inhomogeneous networks.

Acknowledgements

I would like to thank my supervisor for the project, Dr. Jeff Murugan, for being a great motivator and lecturer. I would like to extend my gratitude to my brother, Elijah Roussos, for Python advice and tutoring. I found the project engaging and challenging; I am happy to have had this opportunity.

References

[1] Romualdo Pastor-Satorras (1), and Alessandro Vespignani (2). *Immunization of complex networks.* (1)Departament de Fısica i Enginyeria Nuclear, Universitat Politecnica de Catalunya, Campus Nord, Modul B4, 08034 Barcelona, Spain. (2)The Abdus Salam International Centre for Theoretical Physics (ICTP), P.O. Box 586, 34100 Trieste, Italy, 2008.

[2] Duncan J. Watts, and Steven H. Strogatz . *Collective dynamics of 'small-world' networks.* 'Nature': volume 393, pages 440–442, 1998.

[3] Jeffrey M. Moehlis, *An SIS model* `https://sites.me.ucsb.edu/~moehlis/APC514/tutorials/tutorial_seasonal/node2.html` , 2002.

[4] Duncan J. Watts, and Steven H. Strogatz . *Collective dynamics of 'small-world' networks.* 'Nature': volume 393, pages 440–442, 1998.

[5] Masaaki Ishikawa, *Optimal Strategies for Vaccination using the Stochastic SIRV Model* Graduate School of Science and Engineering, Yamaguchi University, Japan, 2012

[6] Simple Maps, *South African Metropole Data and Populations*, `https://simplemaps.com/data/za-cities`

[7] Towards Data Science, *Easy Steps To Plot Geographic Data on a Map in Python* `https://towardsdatascience.com/easy-steps-to-plot-geographic-data-on-a-map-python-11217859a2db`

[8] Open Street Map, *South African Map* `https://www.openstreetmap.org/export#map=5/-28.613/24.675`

[9] Johns Hopkins, Bloomberg School of Public Health, *Why COVID-19 Vaccines Offer Better Protection Than Infection*, `https://publichealth.jhu.edu/2021/why-covid-19-vaccines-offer-better-protection-than-infection`

[10] Albert-Laszlo Barabasi, *Network Science: Random Networks*, `https://barabasi.com/f/624.pdf`

[11] Mathematical Association of America, *The SIR Model for Spread of Disease - The Differential Equation Model*, `https://www.maa.org/press/periodicals/loci/joma/the-sir-model-for-spread-of-disease-the-differential-equation-model`

Appendix

Province	Province Capitals	Cities in Province
Gauteng	Pretoria	Vereeniging
	Johannesburg	Carletonville
		Randburg
		Centurion
		Sandton
		Springs
		Benoni
		Roodepoort
		Alberton
		Vanderbijlpark
		Brakpan
KwaZulu-Natal	Pietermaritzburg	Ulundi
		Vryheid
		Durban
		Port Shepstone
		Ladysmith
Free State	Bloemfontein	Welkom
		Kroonstad
Eastern Cape	Bhisho	East London
		Umtata
		Port Elizabeth
		Jeffrey's Bay
		Queenstown
		Uitenhage
		Grahamstown
		Graaff-Reinet
		Aliwal North
		Cradock
Limpopo	Polokwane	Lebowakgomo
		Thohoyandou
		Tzaneen
		Musina
North West	Mahikeng	Klerksdorp
		Potchefstroom
		Brits
		Rustenburg
		Mmabatho
		Vryburg
		Lichtenburg
		Mahikeng
Western Cape	Cape Town	Hermanus
		George
		Paarl
		Worcester
		Saldanha
		Oudtshoorn
		Mossel Bay
		Knysna
		Kuilsrivier
		Beaufort West
		Vredenburg
		Malmesbury
Mpumalanga	Nelspruit	Middelburg
		Bethal
		Standerton
		Volksrust
Northern Cape	Kimberley	De Aar
		Upington